

2/12/2018

---

---

---

# Small-scale demo of two CSGRIP containers

---

---

---

Redouane Eddeane  
Seungyeon Kim

# Small-scale demo of two CSGRIP containers

- 1 Vision and outlook of the Smart Energy Delivery lab (SEND LAB) ..... 2
  - 1.1 Introduction..... 2
  - 1.2 Smart Energy Delivery lab ..... 2
- 2 Small-scale demo of two CSGRIP containers ..... 5
  - 2.1 Introduction ..... 5
  - 2.2 Set up of small-scale demo of two containers ..... 5
    - 2.2.1 General description ..... 5
    - 2.2.2 Two microgrid network configurations for simulations..... 7
    - 2.2.3 Two microgrid network configurations for experimental analysis ..... 8
  - 2.3 Preliminary tests and results..... 11
    - 2.3.1 Test scenarios ..... 11
    - 2.3.2 Simulation results..... 12
    - 2.3.3 Experimental results..... 12
- 3. Conclusions ..... 17
- References ..... 19

# 1 Vision and outlook of the Smart Energy Delivery lab (SEND LAB)

---

## 1.1 Introduction

A common challenge in moving from a simulation environment to hardware is the simulation model does not capture all of the intricacies of a hardware implementation. For example, parametric uncertainty in the system will result in incorrect operations and could damage the system without appropriate protection mechanisms. Another challenge when transitioning from simulation to real-world hardware is modeling the interaction and controls between multiple microgrids and accounting for the necessary communications, protection, and controls required to prevent equipment failure and blackout. This risk can be mitigated by performing initial technology development utilizing a flexible and reconfigurable low-power hardware testbed. A historical example of a hardware testbed for power systems can be found in an application from the 1970s which involved using an analog grid simulator to develop controls for a FACTS (Flexible Alternating Current Transmission System) system.

Beside above mentioned challenges, Electrical engineering and in particular electrical energy education are facing a lot of challenges. The number of student who choose electrical engineering is decreasing. Electrical energy is everywhere and due to energy transition is the need of electrical engineers increasing. There is a need of a flexible Energy lab platform where students, teachers and researchers can do experiments to link theory to the practice.

The Smart Energy Delivery lab platform (SEND lab) will be proposed and discussed for above described purpose.

One of the main goal of this SEND lab is to visualize and concretize the Smart Energy research and education within the electrical engineering education.

## 1.2 Smart Energy Delivery lab

The SEND lab design is a low-voltage micro-grid that utilizes low-power versions of the devices implemented in a real-world micro-grid. communications from the SEND lab are directly transferable with implementation. Low voltage and power prototyping allows for direct access and hands on development without the fear of significant electrical shock and destruction of expensive equipment. This accelerates the execution and transition of microgrid-related science from the lab into the field by helping to alleviate many of the challenges of full power control development including tuning of control interactions. Areas that this platform hopes to support include: addressing networked microgrid control and optimization, standardization and including renewables and energy storage, different types of loads, such as buildings, equipment, appliances, and vehicles, protection, communications, and cyber-physical security.

The first generation of SEND lab will be composed of full electronics (NI) hardware controllers, battery energy storage, generators, and load at interconnection voltage of 24 VAC 3-phase as shown in figure 1. This system supported rapid prototyping and quick of energy storage and microgrid controls to full power systems.

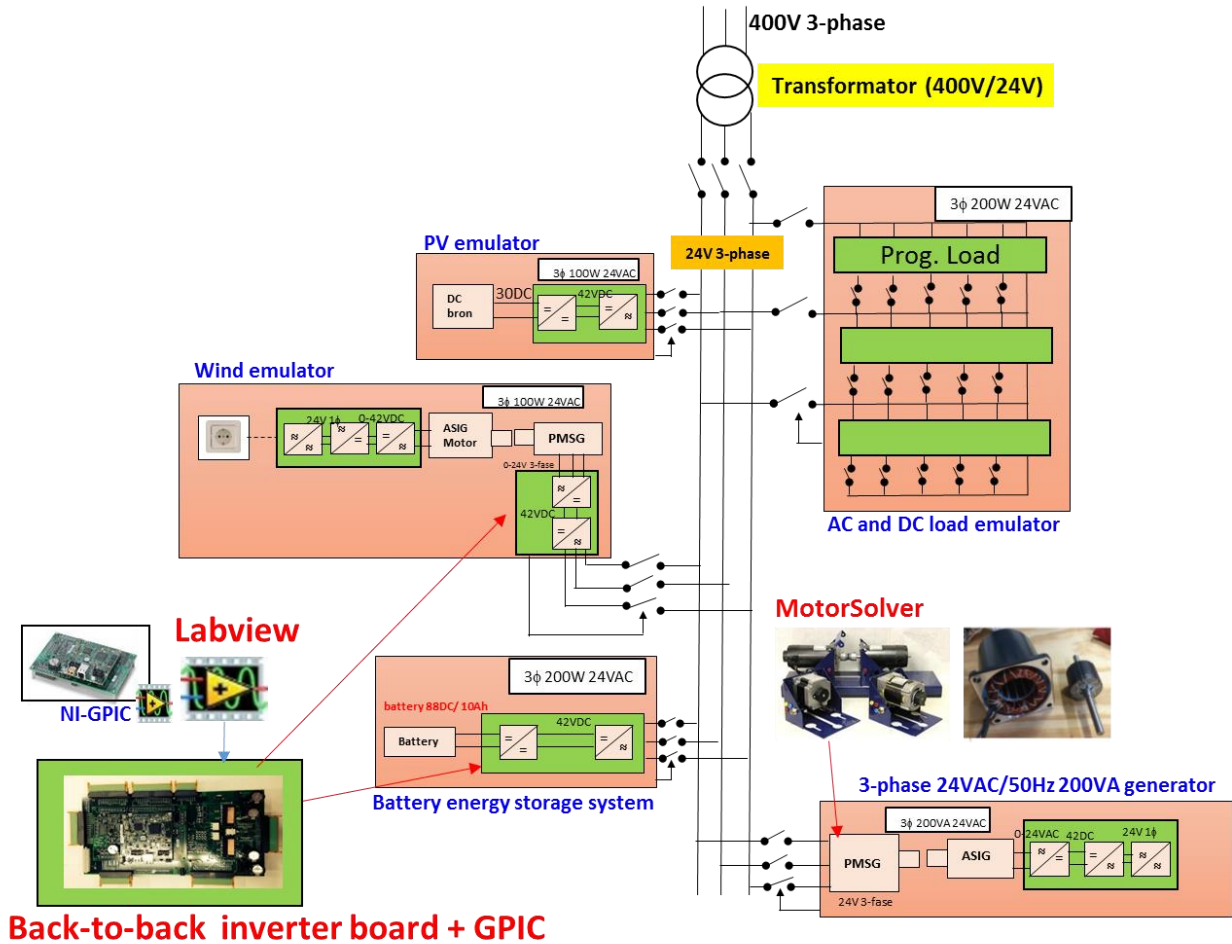


Figure 1: SEND lab hardware setup

This microgrid testing platform is based on NI General Purpose Inverter Controller (GPIC) [1] paired with open source GPIC back-to-back inverter 3-phase control development systems[2]. These converter platforms allow full-scale control development and testing at low current levels. These control development systems contain 2 integrated circuit each with a 3-legged converter as shown in figure 2. These converters can be used either as inverters, rectifiers, or DC/DC converters by adding filtering or boosting inductors at the input/out of the converter. The integrated circuits will support currents up to 10A peak and 5Arms continuous per phase. This provides the flexibility to create several device configurations and system designs utilizing a single design package. During the first phase development, the DC/DC converter controls and the inverter controls were often deployed on two separate Control Development systems due to the limited size of FPGA on the sbRIO. Future designs will utilized the CompactRIO with much larger FPGA and also a new generation of the sbRIO has been released to include a larger FPGA.

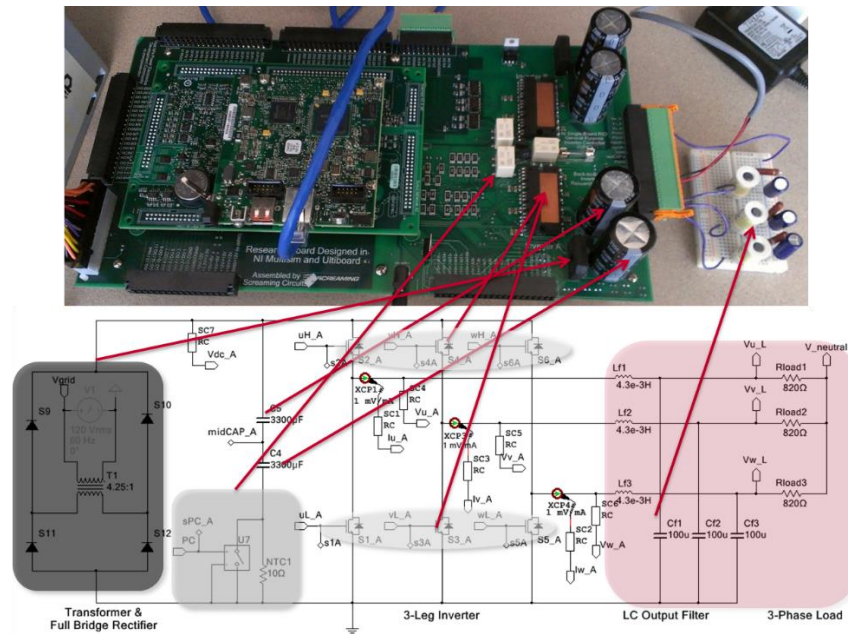


Figure 2: Three phase back-to-back control development system

A second generation SEND lab will allow for a more flexible and larger framework of testing. This future SEND lab will consist of a network of multiple fully functioning reconfigurable low- voltage microgrids as shown in figure 3. Some of the anticipated features of the platform include:

1. complies with relevant standards existing and under development;
2. is extensible by interfacing to grid simulators existing and under development;
3. employs an open data architecture;
4. generates data sets for advanced grid research and
5. can be used to establish/host grid resiliency/cyber-security war games exercises.

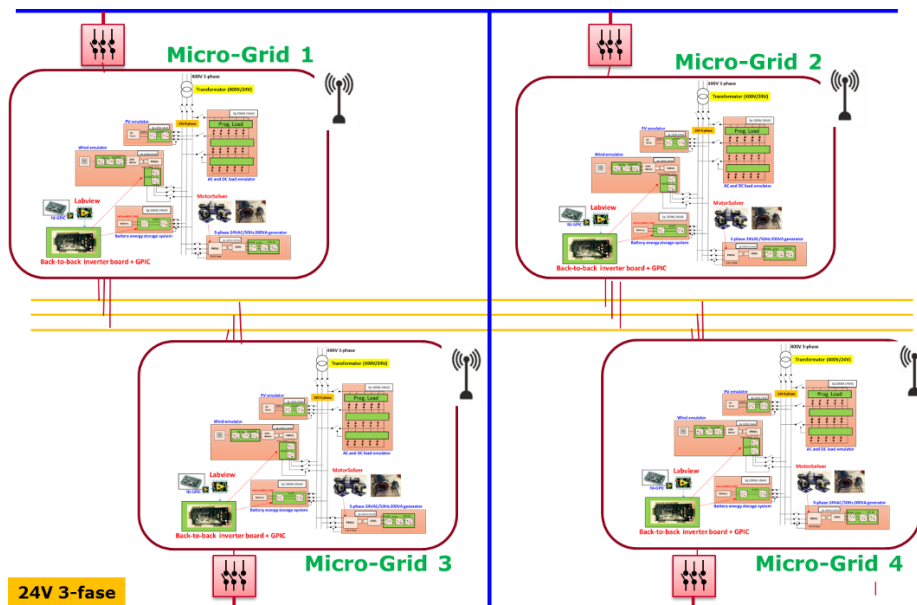


Figure 3: Network of multiple microgrids

## 2 Small-scale demo of two CSGRIP containers

### 2.1 Introduction

This chapter aims to describe the design and implementation of two microgrid systems as a part of the SEND lab described in chapter 1. The performed experiments will prove the concept of the interconnected microrgrids with no connection to the conventional electrical grid, that use dynamic droop curves as the only means of communication as Developed on the CSGRIP project. Moreover, the developed system will also include necessary controllers that will enable smooth transfer between different operational modes. The controllers will show increased performance compared to the previously developed ones, increasing the overall dynamic stability of the system. In summary, the main contributions are as follows:

- A new synchronisation method using Synchronous Reference Frame-Phase Locked Loop (SRF-PLL) will be developed; introducing phase angle detection and calculation in the system will significantly improve synchronization performance,
- A novel fuzzy controller is devised that helps to establish dynamic stability of the droop controller, and thus will enable stable disconnection of a microgrid,
- The performance of both enhanced droop control as well as the developed fuzzy controllers will be validated by both simulations and experiments.

### 2.2 Set up of small-scale demo of two containers

#### 2.2.1 General description

The microgrid to be developed is interfaced with a Voltage Source Inverter (VSI) and a battery management system(BMS); it is connected to local loads, and DGs such as PV and wind, forming into a cell. The architecture of a single cell is depicted in figure 4.

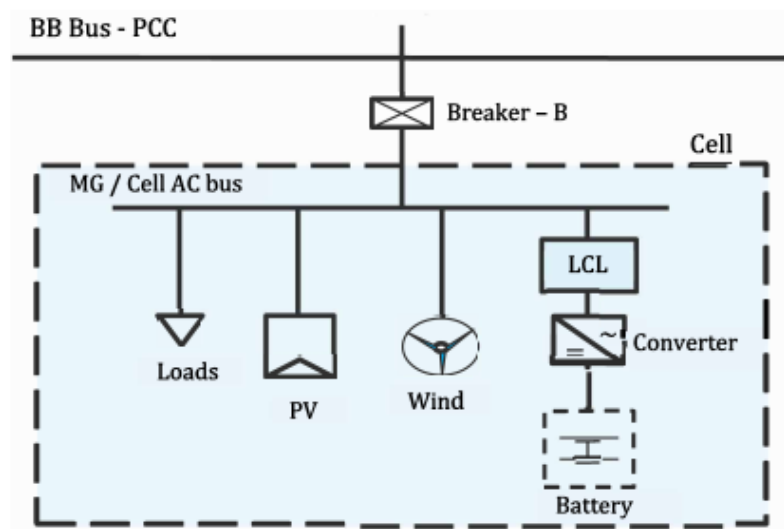


Figure 4: Microgrid architecture [3]

As can be seen in the figure, the cell is linked to the backbone through an electrical switch, namely, circuit breaker. The circuit breaker is utilized to either isolate or connect the microgrid to the backbone. The same architecture can be applied to multiple cells, making them an interconnected system, which is the main idea of the CSGriP project. The schematic of the interconnected cells is presented in figure 5.

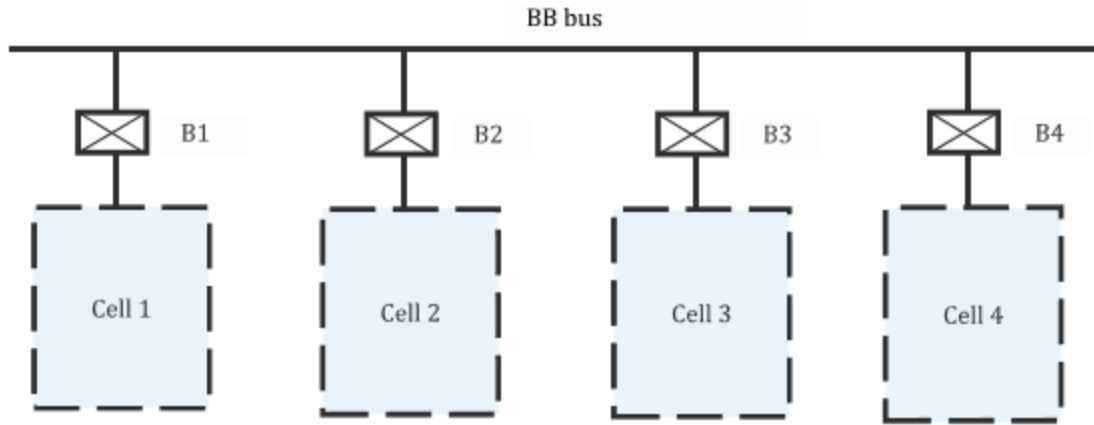


Figure 5: Interconnected multiple microgrids through backbone [3]

This figure is just to give some ideas on the interconnected cells, the number of connected cells can certainly be increased or decreased according to the system's needs.

Labview is a widely used software in industries for testing, control, and measurements. The built-in functions and tools of Labview allow simple programming which then can be directly tested with hardware. In this research, National Instrument's GPIC(General Purpose Inverter Control) FPGA (Field Programmable Gate Array) board is used for hardware implementations. Labview also allows co-simulation with a virtual power electronics circuit. The virtual circuit created in NI multisim resembles that of a real-life hardware; the behavior is also expected to be similar, thus it is an effective tool to make comparison between simulations and experimental results. Figure 6 shows the graphical overview of how co-simulations are conducted. Two virtual instruments on the left hand side represent FPGA board. FPGA board can be considered as the central brain of the mirogrids; they contain all the necessary controllers and feed required output signal to the interfaced DC/AC converter. For simulations, a virtual circuit is drawn using Multisim. Multisim gives the freedom to choose power electronics components that suit the best for operation of the system. In order to achieve clear comparison between simulation and experimental results, all the component values required for a microgrid system, such as LCL filter and loads, were the same as the real-life hardware.

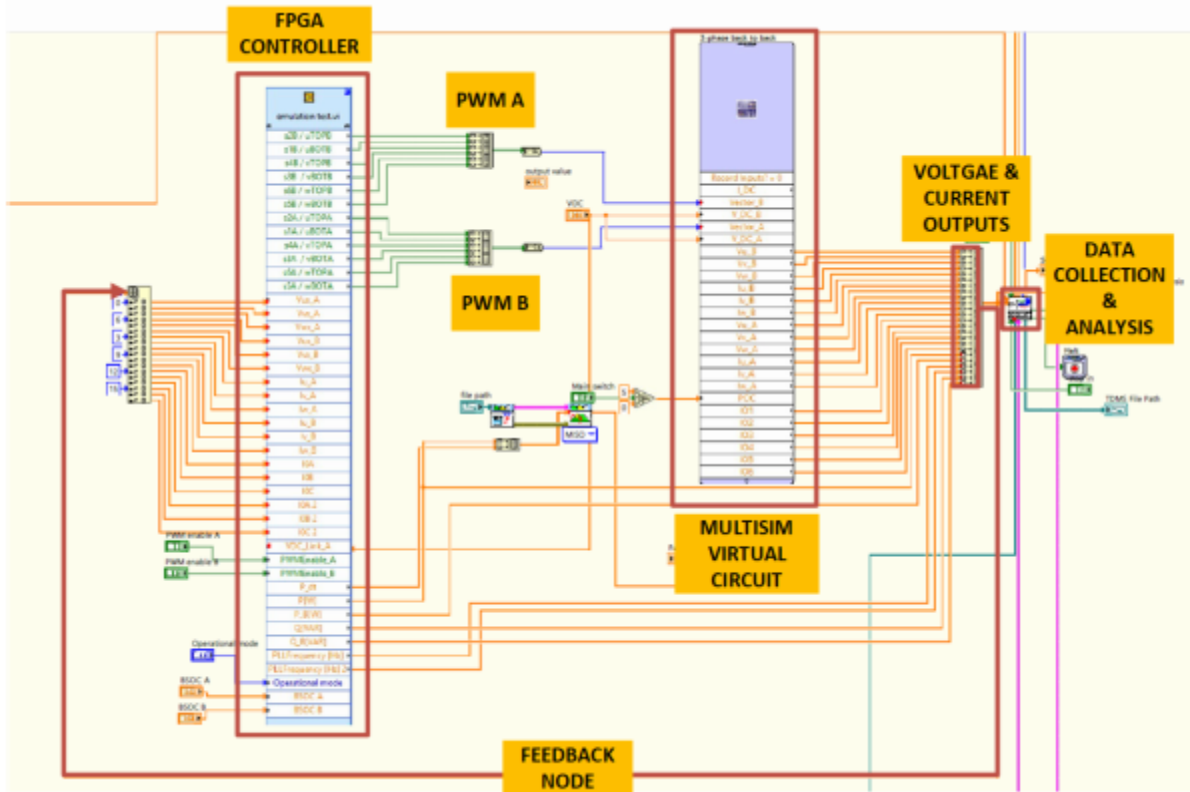


Figure 6: Schematic diagram of a voltage source inverter

For simulations and experimental analysis, a two microgrid network connected through a backbone is designed [4]. This section will be divided into two subsections. The first subsection describes the design of the virtual network used for co-simulations. Next, the network configuration for the experimental setup will be given. Note that here, the same configuration is adapted for both analysis. For the experimental analysis, the overall layout of the experimental system will also be included.

### 2.2.2 Two microgrid network configurations for simulations

In the case of simulations, the controller is connected to a virtual network, as depicted in figure 7. There are two 3-phase DC/AC inverters each containing six IGBT switches. The switches operate according to the PWM signals fed from the FPGA controller. They are connected through a relay switch, of which can be controlled through the FPGA to be switched on or off. A backbone is emulated through connection of AC lines with impedance. The loads of the each inverter is connected through this backbone, making it a low voltage network. The placement of probes for voltage and current measurements allow monitoring of the parameters, as well as calculation of instantaneous power.

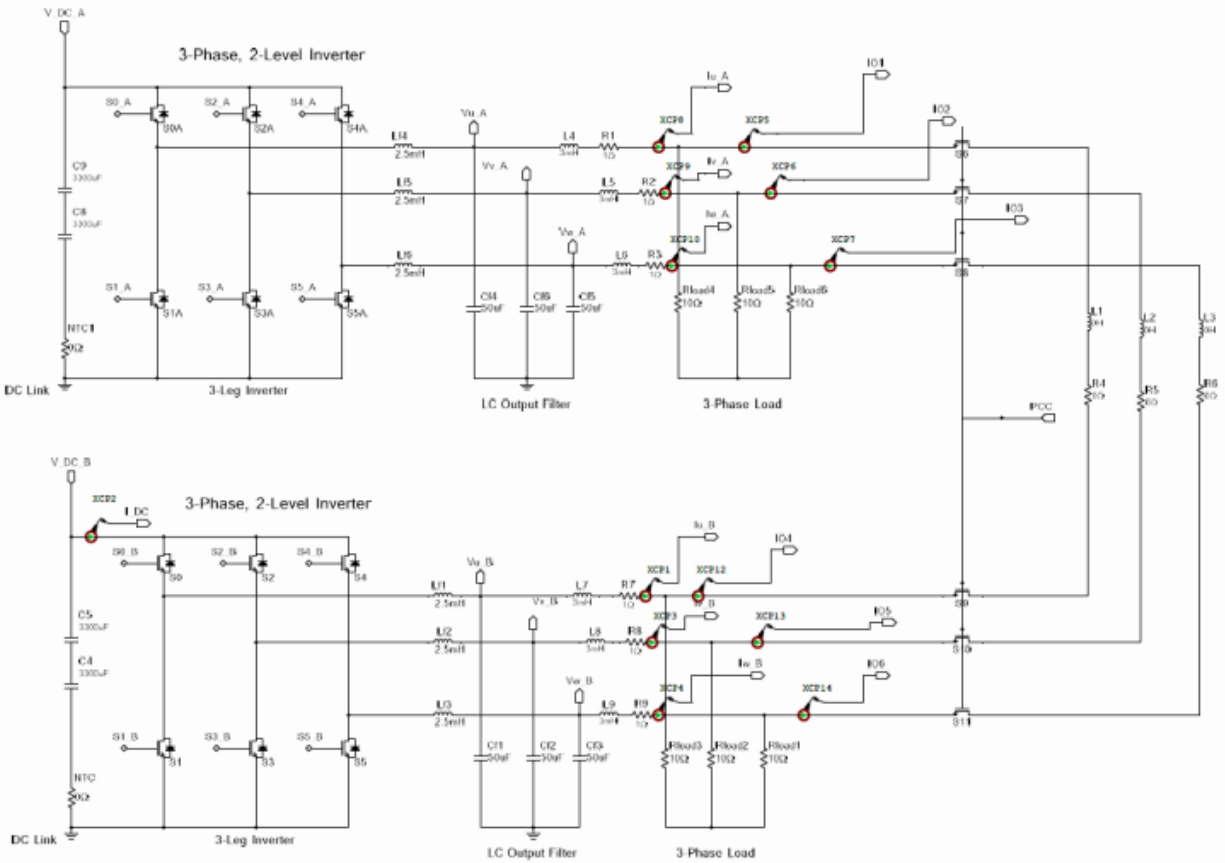


Figure 7: Two microgrid network configurations

### 2.2.3 Two microgrid network configurations for experimental analysis

The GPIC FPGA back-to-back inverter board used for experimental analysis is shown in figure 8. This board contains two inverters of which are identical to the ones used for co-simulations. In this figure, one inverter circuit is included as an example. Each arrow in the figure indicates corresponding component of the circuit to the hardware. Using this board, a microgrid network is configured. Figure 9 shows schematic diagram of the configuration used here. The outputs of the inverters are connected to physical filters and loads. Similar to simulations, the loads of each inverter is connected with AC lines, making it a backbone. In this case, a mechanical switch is utilized for linking the two microgrids. This is because some memory issues with the FPGA board was experienced, thus a control layer for switching the systems could not be included in the control loops. For observations of short-term dynamics of the system, it is expected that a mechanical switch would be sufficient. Furthermore, there is an extra control layer in the system determining whether or not the microgrids are ready to be (dis)connected. The FPGA board not only includes inverters used for microgrid interfaces, but also is compiled with all the necessary controllers developed in a host computer. During experiments, the FPGA sends PWM and other control signals to the two built-in inverters. The output of the inverters are consumed by the filters and loads connected, and those signals are collected back to the FPGA, making a closed loop system.

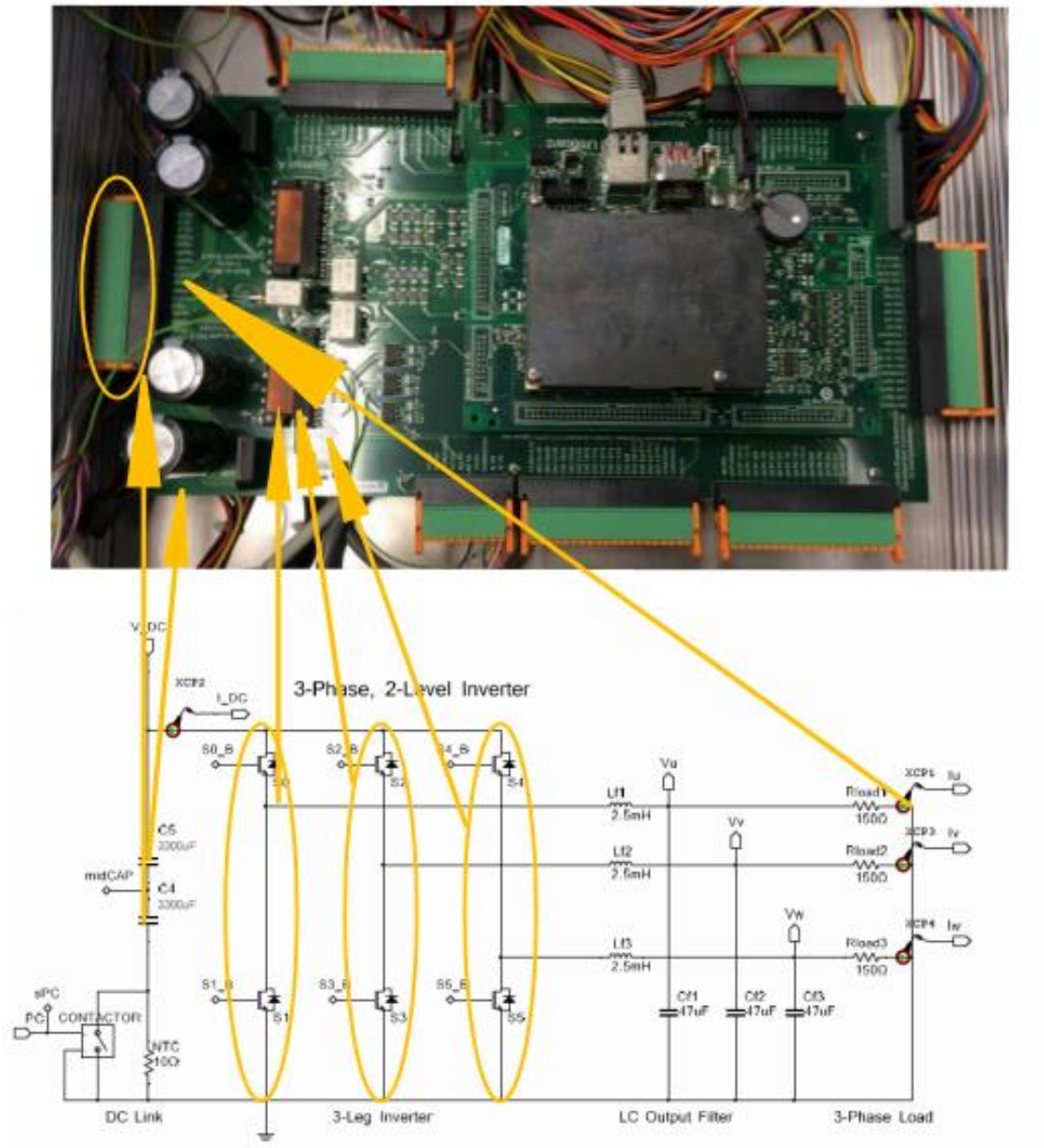


Figure 8: Hardware set up for two microgrid network configurations

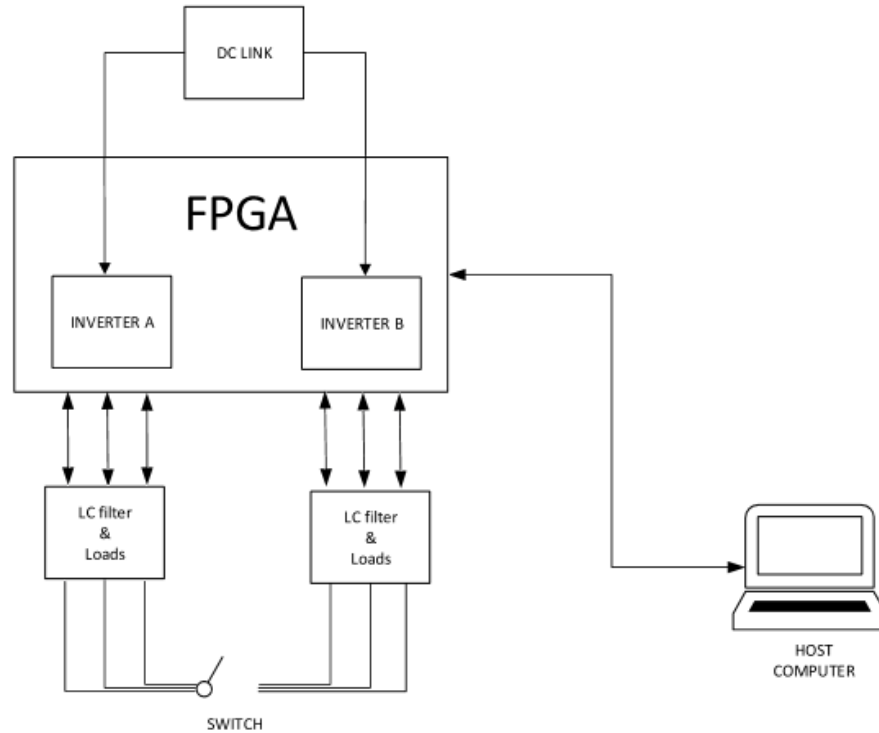


Figure 9: System configuration of the experimental set up

The actual experimental set up is shown in figure 10. The set up was made based on the configuration drawing in figure 7. It is clear in this figure, that all the mentioned components are formed into a network. This will allow to test the controller in a similar environment to simulations.

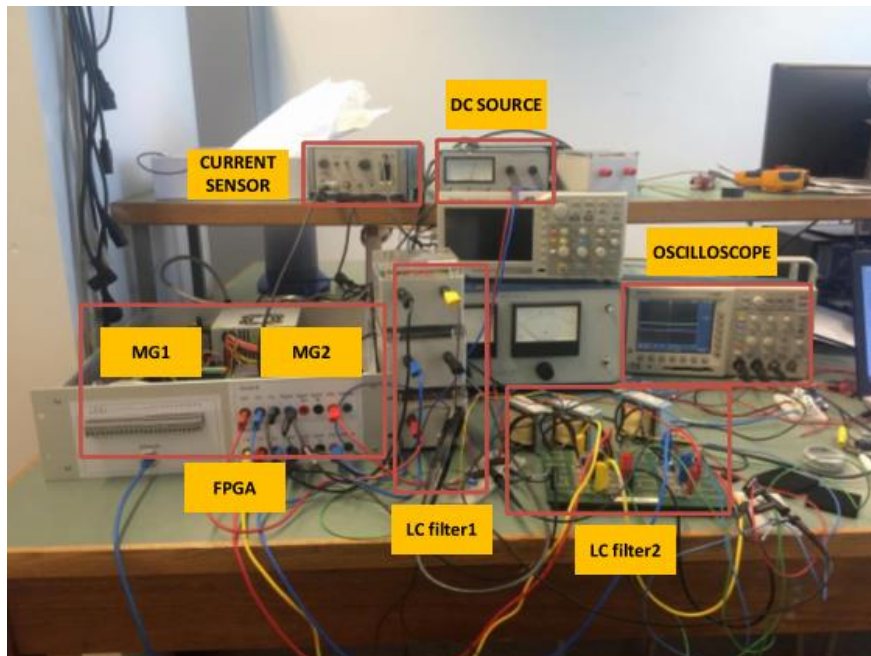


Figure 10: Experimental set up for the two interconnected microgrids

## 2.3 Preliminary tests and results

### 2.3.1 Test scenarios

In this section, the test scenarios for simulations and experimental analysis will be given. Note here that, to achieve clear comparisons, similar conditions will be used for both analysis. Due to hardware limitations, the exact same parameters could not be used; the values will be scaled down for safe operation of the experimental demonstrations. The scenarios will be divided into two parts, namely base case and transient case. The base case would be the testing of general behaviors of the developed controllers. This will include power sharing, synchronization and intentional disconnection. These controllers are typically considered to be less challenging than unintentional islanding process. Therefore, only a single base case will be demonstrated for these general scenarios. The performance of new controllers will be evaluated and compared to the previous works. The latter case, will focus on the more challenging control, which is to minimize transients during unintentional islanding. In order to prove the performance of the developed controllers, this section will first examine transient behaviors of two microgrids without any extra disconnection controller implemented. Amongst the tested scenarios, the worst one will be chosen, and then will be used as the base case for evaluating the performance of the fuzzy disconnection controller.

The scenarios mentioned so far, for both simulations and experiments are summarized in table 1. The testing of the scenarios are going to be conducted in the order of the lists. Results and discussion of the outcomes will be presented and analyzed in the coming chapters. From here on, base and transient cases will be referred to as BC and TC respectively. The corresponding names for seamless transition cases: connection, intentional disconnection and unintentional disconnection will be C, ID and UD. These names will be paired with case numbers defined earlier, and will be written in the remark section in the scenario description tables.

Table 1: Conditions for test scenarios

|                 | Scenario | SOC [%] |     | $P_{demand,sim.}$<br>[W] |     | $P_{demand,exp.}$<br>[W] |      | Droop gain<br>[Hz/W] | Remark    |
|-----------------|----------|---------|-----|--------------------------|-----|--------------------------|------|----------------------|-----------|
|                 |          | MG1     | MG2 | MG1                      | MG2 | MG1                      | MG2  |                      |           |
| Base cases      | 1        | 30      | 50  | 15                       | -15 | 2.5                      | -2.5 | 0.01~0.07, fuzzy     | BC-Droop  |
|                 | 2.1      | 30      | 50  | 5                        | 5   | 1                        | 1    | Fuzzy                | BC-C1     |
|                 | 2.2      | 20      | 80  | 5                        | 5   | 1                        | 1    | Fuzzy                | BC-C2     |
|                 | 2.3      | 20      | 60  | 5                        | 5   | 1                        | 1    | Fuzzy                | BC-C3     |
|                 | 3.1      | 30      | 50  | 15                       | -15 | 2.5                      | -2.5 | Fuzzy                | BC-ID1    |
|                 | 3.2      | 20      | 80  | 15                       | -15 | 2.5                      | -2.5 | Fuzzy                | BC-ID2    |
|                 | 3.3      | 20      | 60  | 15                       | -15 | 2.5                      | -2.5 | Fuzzy                | BC-ID3    |
|                 | 3.4      | 30      | 50  | 5                        | -5  | 1.5                      | -1.5 | Fuzzy                | BC-ID4    |
|                 | 3.5      | 30      | 50  | 10                       | -10 | 2.5                      | -2.5 | Fuzzy                | BC-ID5    |
|                 | 3.6      | 30      | 50  | 15                       | -15 | 3.5                      | -3.5 | Fuzzy                | BC-ID6    |
| Transient cases | 4        | 30      | 50  | 15                       | -15 | 2.5                      | -2.5 | 0.01~0.07, fuzzy     | TC-UD-4   |
|                 | 5.1      | 30      | 50  | 5                        | -5  | 1.5                      | -1.5 | Fuzzy                | TC-UD-5.1 |
|                 | 5.2      | 30      | 50  | 10                       | -10 | 2.5                      | -2.5 | Fuzzy                | TC-UD-5.2 |

|  |     |    |    |    |     |     |      |       |           |
|--|-----|----|----|----|-----|-----|------|-------|-----------|
|  | 5.3 | 30 | 50 | 15 | -15 | 3.5 | -3.5 | Fuzzy | TC-UD-5.3 |
|--|-----|----|----|----|-----|-----|------|-------|-----------|

### 2.3.2 Simulation results

In this chapter, a total of five scenarios are evaluated through simulations in LabVIEW. The first three included general cases, testing performances of synchronization and intentional islanding controllers. The rest of the scenarios are going to demonstrate transient cases induced by an unintentional disconnection.

#### **SCENARIO 1 - POWER SHARING PERFORMANCE BASED ON DROOP GAINS**

From the obtained simulation results, it is concluded that the use of higher droop gain decreases system stability, but also increases response time for power demand changes. The employment of the fuzzy droop gain showed good performance in terms of both stability and response time.

#### **SCENARIO 2 - TRANSITION FROM ISLANDED TO BACKBONE CONNECTED MODE**

From the results obtained in scenario 2, it can be concluded that the synchronization controller developed in this thesis works for all values of SOC. The performance of the controller has also been improved from the previous one, showing 95 % better performance in synchronization time.

#### **SCENARIO 3 - INTENTIONAL ISLANDING**

To conclude, the disconnection controller was successful in reducing the line power to zero in different values of SOC and  $\Delta P$ . It was seen that SOC of the microgrids had minor influence on the preparation time for the disconnection. On the other hand, the magnitudes of  $\Delta P$  were found to have an influence on the controller performance. Furthermore, the disconnection time for the new controller showed 94 % better performance compared to the previous one.

#### **SCENARIO 4 - THE EFFECT OF DROOP GAINS (Transient behaviors)**

To summarize, the largest overshoot of 1.5 % was found with the droop gain of 0.07, which was the highest droop gain used in this scenario. For the lowest droop gain, the overshoot just remained 0.24 %. The fuzzy droop gain showed damped response during the unintentional islanding. From these results, it can be concluded that the fuzzy droop controller showed good performance in reducing sudden transients during an unintentional islanding.

#### **SCENARIO 5 - FUZZY DROOP CONTROLLER - THE INFLUENCE OF EXCHANGED POWER**

In regards to the influence of different values of  $\Delta P$ , the higher value of  $\Delta P$  resulted in more deviation in the active power output. However, unlike a constant droop gain response, the frequency outputs in all cases showed damped response. From these results, it can be concluded that the fuzzy droop controller can effectively reduce sudden transients in different ranges of exchanged power between microgrids.

### 2.3.3 Experimental results

In this chapter, the results obtained for experimental analysis will be presented. Similar to simulation results, the chapter will start with giving results for base cases. These cases will evaluate general performances of the controllers developed. Then the chapter is followed by experimental analysis of seamless controllers developed in this study.

#### **SCENARIO 1 - DROOP CONTROL**

The experimental results for power sharing performance are given in this section. The performance was evaluated based upon different droop gains; test method and droop gains used here are the same as simulation scenario 1. Table 2 lists the test conditions used in this scenario. At 0 second, two microgrids are already synchronized and connected. There is no exchanged active power between the microgrids at the start of the experiments. At 1 second, MG1 reduces its load active power consumption to 5 [W]. According to the droop equation, this causes frequency increase in MG1, resulting in active power flow from MG1 to MG2. The frequency is eventually eliminated once both systems reach steady state.

Table 2: Test condition for scenario 1

| Scenario | SOC [%] |     | $P_{demand}$ [W] |     | $Q_{demand}$ [VAR] |     | Droop gain [Hz/W] |
|----------|---------|-----|------------------|-----|--------------------|-----|-------------------|
|          | MG1     | MG2 | MG1              | MG2 | MG1                | MG2 |                   |
| 1        | 30      | 50  | 5                | -5  | 0                  | 0   | 0.01              |
|          | 30      | 50  | 5                | -5  | 0                  | 0   | 0.03              |
|          | 30      | 50  | 5                | -5  | 0                  | 0   | 0.05              |
|          | 30      | 50  | 5                | -5  | 0                  | 0   | 0.07              |
|          | 30      | 50  | 5                | -5  | 0                  | 0   | 0.2               |
|          | 30      | 50  | 5                | -5  | 0                  | 0   | Fuzzy             |

the trend in frequency response is similar to that of simulation results: a larger steady-state oscillation and faster response time were found among higher droop gains, and vice-versa for lower gains. The response time and oscillation level for each droop gain are tabulated in table 3. In order to make comparisons, the simulation results are included in the table as well.

Table 3: Droop gain vs. steady state time

| Droop gain | Response time [s] |      | Oscillation level [%] |      |
|------------|-------------------|------|-----------------------|------|
|            | Sim.              | Exp. | Sim.                  | Exp. |
| 0.01       | 0.5               | 1.8  | 0.07                  | 0.01 |
| 0.03       | 0.168             | 1    | 0.19                  | 0.03 |
| 0.05       | 0.115             | 0.4  | 0.35                  | 0.06 |
| 0.07       | 0.08              | 0.3  | 0.49                  | 0.1  |
| 0.2        | -                 | 0.1  | -                     | 0.2  |
| Fuzzy      | 0.115             | 0.35 | 0.14                  | 0.03 |

The trend is more visible in table 3. The response time was the slowest for droop gain 0.01; it took 1.8 s for two microgrids to reach steady state. In regards to oscillation level, the oscillation was the highest for droop gain 0.2, where it showed oscillation of 0.14% from its calculated steady state value. Although the same trend was found among the simulation and experimental results, the actual values of the results were very different. For example, the response time with fuzzy droop gain in the simulation was 0.115 s, whereas in the experiment, it was 0.35 s. The same goes for oscillation level as well; the deviations for fuzzy droop gain were 0.14% and 0.03% in the simulation and experiment respectively. In general, faster

response time were found in the simulations and the oscillation levels were lower in the experiments. A possible reason for such differences could be the heavy usage of digital filters during the experiments. The filters were used for power calculations, as the signals after the physical filters were not obtainable. The usage of filters could have resulted in slower, but also more stable system.

### SCENARIO 2 - FROM ISLANDED TO BACKBONE CONNECTED MODE

The synchronization controller for various values of SOC are experimentally validated in this section. At the start of the experiments, two microgrids are operated independently. At  $t=1$  s, synchronization controller is activated at the microgrid with a lower SOC. The controller tries to reduce frequency, voltage and phase angle error between two microgrids to the specified limits. The test conditions for this scenario are listed in table 4. For fair comparisons, the similar conditions were adapted as the simulation scenario 2.

Table 4: Test conditions for scenario 2

| Scenario | Case | SOC [%] |     | $P_{demand}$ [W] |     | $Q_{demand}$ [VAR] |     | Droop gain [Hz/W] |
|----------|------|---------|-----|------------------|-----|--------------------|-----|-------------------|
|          |      | MG1     | MG2 | MG1              | MG2 | MG1                | MG2 |                   |
| 2        | 1    | 30      | 50  | 5                | 5   | 0                  | 0   | Fuzzy             |
|          | 2    | 20      | 80  | 5                | 5   | 0                  | 0   | Fuzzy             |
|          | 3    | 20      | 60  | 5                | 5   | 0                  | 0   | Fuzzy             |

From table 5, it can be seen that the influence of different values of SOC on the synchronization time is minor. Instead, the initial phase angle difference before synchronization were found to be the core influence on the controller performance. The longest synchronization time was found in case 1, where the phase angle difference was 2.25 rad. In fact, this is the same trend as the simulation results. For both analysis, similar values among synchronization time and initial phase angle difference were observed. For example, for simulation case 1, synchronization time and phase angle difference were 2.9 s and 2.9 rad respectively. The experimental result showed 2.5 s and 2.25 rad for the same parameters.

Table 5: Synchronization time comparisons for simulation and experiment

| Case | SOC [%] |     | Sync. time [s] |      | Init. Phase angle difference [rad] |      |
|------|---------|-----|----------------|------|------------------------------------|------|
|      | MG1     | MG2 | Sim.           | Exp. | Sim.                               | Exp. |
| 1    | 30      | 50  | 2.9            | 2.5  | 2.9                                | 2.25 |
| 2    | 20      | 80  | 0.6            | 2    | 0.6                                | 1.8  |
| 3    | 20      | 60  | 3              | 1.8  | 2.95                               | 1.5  |

### SCENARIO 3 - INTENTIONAL ISLANDING

The experimental results for scenario 3, where the islanding process is planned, are given in this section. The two microgrids are initially interconnected, and a designated amount of active power is being exchanged between them. At 1 s, the microgrids starts preparing for the islanding process by reducing the

exchanged active power to zero. For this scenario, the influence of different values of SOC and active power demand are evaluated. The results will be compared to that of the simulation results. Table 6 enlists the test conditions used for this scenario.

Table 6: Test conditions for scenario 3

| Scenario | Case | SOC [%] |     | $P_{demand}$ [W] |      | $Q_{demand}$ [VAR] |     | Droop gain [Hz/W] |
|----------|------|---------|-----|------------------|------|--------------------|-----|-------------------|
|          |      | MG1     | MG2 | MG1              | MG2  | MG1                | MG2 |                   |
| 3.1      | 1    | 30      | 50  | 2.5              | -2.5 | 0                  | 0   | 0.05              |
|          | 2    | 20      | 80  | 2.5              | -2.5 | 0                  | 0   | 0.05              |
|          | 3    | 20      | 60  | 2.5              | -2.5 | 0                  | 0   | 0.05              |
| 3.2      | 1    | 30      | 50  | 1.5              | -1.5 | 0                  | 0   | 0.05              |
|          | 2    | 30      | 50  | 2.5              | -2.5 | 0                  | 0   | 0.05              |
|          | 3    | 30      | 50  | 3.5              | -3.5 | 0                  | 0   | 0.05              |

The influence of SOC on the performance of the disconnection controller was close to zero. The exchanged active power  $\Delta P$  on the other hand, showed large influences on the preparation time for disconnection. Table 7 shows the disconnection time for each case, including the results obtained from simulation scenarios as well.

Table 7: Disconnection time during intentional islanding

| Scenario | Case | SOC [%] |     | $\Delta P$ [W] |      | Discon. time [s] |      |
|----------|------|---------|-----|----------------|------|------------------|------|
|          |      | MG1     | MG2 | Sim.           | Exp. | Sim.             | Exp. |
| 3.1      | 1    | 30      | 50  | 2.5            | 15   | 0.15             | 1    |
|          | 2    | 20      | 80  | 2.5            | 15   | 0.138            | 1    |
|          | 3    | 20      | 60  | 2.5            | 15   | 0.14             | 1    |
| 3.2      | 1    | 30      | 50  | 1.5            | 5    | 0.13             | 0.8  |
|          | 2    | 30      | 50  | 2.5            | 7.5  | 0.1375           | 1    |
|          | 3    | 30      | 50  | 3.5            | 15   | 0.15             | 1.2  |

The trend for SOC and  $\Delta P$  influences on the controller performance was found to be the same for both analysis. However, experimental results showed 86% slower response compared to that of simulation results. The same possible reason could be adapted here as well: the use of the digital filters could have slowed down the whole control process.

#### SCENARIO 4 - THE EFFECT OF DROOP GAINS ON TRANSIENT BEHAVIOR

In this experiment, the MG 1 was injecting active power of 2.5 W to the MG 2. At 1 s, a fault occurs in the system, and two microgrids are suddenly disconnected. In this scenario, the influences of the different droop gains will be evaluated. The droop gains used here are : 0.01, 0.03, 0.05, 0.07, 0.2 and fuzzy gain. The test conditions for this scenario are listed in table 8.

Table 8: Test conditions for scenario 4

| Scenario | Case | SOC [%] |     | $P_{demand}$ [W] |      | $Q_{demand}$ [VAR] |     | Droop gain [Hz/W] |
|----------|------|---------|-----|------------------|------|--------------------|-----|-------------------|
|          |      | MG1     | MG2 | MG1              | MG2  | MG1                | MG2 |                   |
| 4        | 1    | 30      | 50  | 2.5              | -2.5 | 0                  | 0   | 0.01              |
|          | 2    | 30      | 50  | 2.5              | -2.5 | 0                  | 0   | 0.03              |
|          | 3    | 30      | 50  | 2.5              | -2.5 | 0                  | 0   | 0.05              |
|          | 4    | 30      | 50  | 2.5              | -2.5 | 0                  | 0   | 0.07              |
|          | 5    | 30      | 50  | 2.5              | -2.5 | 0                  | 0   | Fuzzy             |

In this experiment, no disturbances were observed during the disconnection. This may be due to the digital fitters used for power measurements, since voltage and current information after physical filters were unavailable. Because of this, changes in voltage and current may not have been captured in the monitoring system, resulting in smooth transitions.

### 3. Conclusions

---

An outlook and vision of the Smart Energy lab (SEND lab) have been discussed. This SEND lab platform will enable a new paradigm in regards to testing of microgrid controls which will enable testing of local controls, system controls, and also producing reference test results in order to benchmark configurations. It will also enable the analysis of both physical measurements and the communications between devices and controls. This type of architecture will allow testing of cyber-attack scenarios and investigation into the impact on microgrids and system control solutions. This SEND lab will also help to increase student who choose power energy and enable a platform where student, teachers and research can do experiments on the area of Smart Energy.

As a part of the SEND lab platform two micorgrids network was built and developed, each of which comprising of a VSI, a battery management system, and loads. No ICT based system is present in the network, and only local measurements are allowed for calculation of the frequency and voltage set points. These set points are calculated through droop control, which is the main idea that dominates the background of CSGRIP project. Droop control utilizes the inductive behavior of line parameters that connect multiple microgrids. This behavior is usually found in medium to high voltage grids, hence a virtual impedance had to be added to emulate this behavior. Concerning the transitions between two operational modes, three controllers were developed. The first controller is responsible for enabling smooth synchronization from islanded microgrid to the backbone. This controller reduces voltage, frequency and phase angle error between two systems within the specified limits. Next, a controller that 'prepares' a microgrid for smooth disconnection from the backbone was implemented. By reducing the exchanged power to zero before disconnection, possible transients could be avoided, and safe disconnection is allowed. Now, these two mentioned controllers were previously developed within the same CSGriP project, but both controllers showed slow performances. Therefore, the focus here was to significantly speed up the synchronization and preparation time. The new controller used Synchronous Reference Frame-Phase Locked Loop(SRF-PLL) method, where it enables simultaneous frequency and phase angle synchronization. Also, fine tuning of the VSI control parameters, that improves the performances of the mentioned controllers was made as well. The third controller is developed for cases where a disconnection is not planned and a micro- grid is disconnected from the backbone due to unexpected events. To minimize transients upon a sudden islanding, fuzzy droop controller was implemented. Fuzzy droop controller was designed based on the fact that transients are highly related to the droop gain chosen for the system. This fuzzy droop controller takes into account the exchanged power  $\Delta P$  and its rate of change  $\Delta dP$  and gives the appropriate droop gain to the system. The gain is designed in such a way that both the fast response time and good stability are realized in the system. To validate and experimentally verify the basic functionality of the developed controllers, several case studies and scenarios were described for both simulations and experiments. The scenarios were divided into two groups: the first group included general performance evaluations of the less challenging controllers. The scenarios in this group include general power sharing performance with different droop gains, synchronization and intentional islanding. The latter group is related to themore challenging control strategy, namely, unintentional islanding. In the first simulated scenario, the influence of droop gains on the power sharing performance was examined. It was noticed that imposing a higher droop gain resulted in better response time, but also decreased the overall stability of the system. The opposite behaviors' were found in the cases with lower droop gains; the system was more stable, but the response was very slow. The results obtained with fuzzy droop gain however, showed good performance in both stability and response time. Similar trends in the results were found among simulation and experimental cases. The performance of the synchronization controller was tested for various values of SOC. The SOC of each

microgrid prior to connection had negligible effect on the synchronization time. In fact, the influence came from the initial phase angle difference between two microgrids. This is due to the fact that phase angle difference is used as an input signal for the controller. Furthermore, the implementation of the SRF-PLL in the synchronization loop showed 70% better performance over the previously developed controller. For this scenario, fair agreements have been found between simulation and experimental results. The relationship between synchronization time and initial phase angle difference were almost the same for both analysis.

In addition, intentional islanding controller under the different values of SOC and exchanged active power,  $\Delta P$  was evaluated. The controller was successful in removing line active power in all cases. The SOC of each microgrid had negligible effect on the preparation time for an intentional islanding. The magnitude of  $\Delta P$  on the other hand, had influences on the controller's performance. The simulation results showed 94% better performance compared to that of the previous controller. Similar relationships were found in the experimental results as well. A small difference in the disconnection time could have resulted from the use of digital filters in the experimental setup. In regards to unintentional islanding scenarios, transients have been found in the cases where a constant droop was used. Here, the similar trend found in power sharing scenario was observed as well: the higher the droop gain, the faster and more unstable the system becomes. The test scenarios where a fuzzy droop gain is applied, showed much more stable disconnection. The same fuzzy droop controller was tested under different  $\Delta P$ . It was shown that the similar damping response was found in all operating cases. The use of digital filters in the experiments resulted in much more stable disconnection in all cases. This means that the design of the fuzzy controller in combination with digital filters would perform even better and more stable in real-life applications.

## References

---

- [1] National Instruments, “NI Single-Board RIO General- Purpose Inverter Controller Features,” <http://www.ni.com/white-paper/14207/en/>, December 2012.
- [2] National Instruments, “GPIC Mini-Scale SKiiP3 Replica Power Converter Control Development System,” <https://decibel.ni.com/content/message/44138>, November 2015.
- [3] Ashil Thomas, A distributive approach of microgrid control based on system frequency, Master’s thesis, TU Delft, 2017.
- [4] Seungyeon Kim, Simulation-based and small lab-scale experimental studies of seamless transitions of two CSGriP cells, Maters’s thesis, TU Delft, 2017